Optical emission from ultrathin strained type-II InP/GaP quantum wells

F. Hatami,[a] G. Mussler, M. Schmidbauer, and W. T. Masselink
Department of Physics, Humboldt-Universität zu Berlin, Invalidenstrasse 110, 10115 Berlin, Germany

L. Schrottke, H.-Y. Hao, and H. T. Grahn
Paul-Drude-Institut für Festkörperelektronik, Hausvogteiplatz 5-7, 10117 Berlin, Germany

(Received 24 May 2001; accepted for publication 5 September 2001)

We describe the growth and optical emission from ultrathin strained InP quantum wells grown on GaP substrates using gas-source molecular-beam epitaxy. The InP thickness was varied between 0.5 and 1.6 monolayers. Intense photoluminescence was emitted from the structures; time-resolved measurements indicate rather long carrier lifetimes of about 19 ns. With decreasing InP coverage, the emission lines are shifted from 2.18 to 2.28 eV due to quantum size effects. We explain the emission as spatially indirect recombination of electrons from the GaP X valleys with holes in InP and its phonon replicas. © *2001 American Institute of Physics.* [DOI: 10.1063/1.1414291]

The development of modern epitaxial growth methods such as molecular-beam epitaxy and metalorganic vapor phase epitaxy in recent years allows the preparation of lattice-mismatched heterostructures with nearly perfect interfaces. Strain changes both the band structure and the discontinuity of the band edges of such systems, resulting in modified optical and transport properties; the additional design freedom won through the incorporation of strained quantum wells (QWs) has resulted in improved semiconductor devices, both optical[1] and electronic.[2]

Two-dimensional (2D), defect-free growth of InP on GaP is limited to very thin layers because of the large lattice mismatch of 7.7% between the two materials. After deposition of about 1.8 monolayers (MLs) of InP, the formation of quantum dots (QDs) via the Stranski–Krastanow mechanism is observed.[3] In the related materials system, $InP/In_{0.48}Ga_{0.52}P$, intense photoluminescence (PL) due to radiative recombination of heavy holes and electrons in both InP QDs as well as in InP QWs embedded in $In_{0.48}Ga_{0.52}P$ is observed at energies between 1.6 and 1.9 eV.[4] Similarly, optical emission from direct-band-gap InP QWs embedded in the indirect GaP matrix is expected to lie between the InP and GaP band gaps. The use of GaP as substrate could take advantage of a well-developed light emitting diode (LED) technology. Furthermore, using transparent GaP rather than GaAs as the substrate allows easier extraction of the emitted light for vertical structures including vertical cavity lasers. Thin InP layers embedded in (100) GaP have been studied using spectroscopic ellipsometry.[5] In the present work, we describe the growth and structural properties of, as well as the strong optical emission from, monolayer InP QWs embedded in a GaP matrix; these results suggest that ultrathin two-dimensional InP layers in GaP form an indirect type-II heterosystem.

The structures were grown by gas-source molecular beam epitaxy (GSMBE) on undoped (100) GaP substrates using a RIBER-32-P MBE system. Prior to growth, the substrates were etched in a solution of $4HCl{:}4HNO_3{:}5H_2O$.[6] After oxide desorption, a 200-nm-thick GaP buffer layer was grown at 500 °C at a rate of 0.9 μm/h. Subsequently, the desired coverage of InP was deposited at a rate of 0.8 MLs/s (0.22 μm/h). We measure the InP coverage in MLs on the GaP surface taking into consideration the enlargement of the vertical InP lattice constant under compressive in-plane strain ($1\,\mathrm{ML}=6.730\times10^{14}$ In atoms/cm^2). Each sample contains nine periods InP/GaP superlattice (SL) with GaP thickness of 4 nm and InP thickness between 0.5 and 1.6 MLs depending on sample. The resulting structures were capped with 10 nm GaP. The growth process was monitored using reflection high-energy electron diffraction (RHEED); during GaP and InP growth, the surface showed a (2×4) reconstruction, indicating 2D growth. The structural properties of the samples were also characterized using double crystal x-ray diffractometry (DCXD) and atomic force microscopy (AFM).

X-ray rocking curves were examined for the (004) reflection using Cu $K\alpha_1$ radiation. The AFM investigations were carried out in a TopoMetrix Discover microscope; these AFM data confirm the absence of islanding in the structures. PL was excited using the 325 nm line of a He–Cd laser; the emission was dispersed in a 1 m monochromator and detected by a charged coupled device (CCD) camera. For the time-resolved PL, the excitation was provided by 400 fs, second harmonic (386 nm) laser pulses of a mode-locked Ti:sapphire laser. A pulse picker reduced the repetition rate from the original 76 MHz to 950 kHz and a Hamamatsu C5680 streak camera was used for detection.

Figure 1 displays experimental (004) rocking curves together with simulations using dynamical diffraction theory. Due to the InP/GaP superlattice, pronounced satellite peaks (denoted as S_{-1}, S_0, and S_1) appear in the proximity of the GaP substrate reflection (denoted as P). The position of the zero-order satellite peak S_0 with respect to P is connected to the mean vertical elastic strain inside the superlattice and, therefore, yields information about the average amount of In. Consequently, S_0 shifts from -1000 to -2000 arcsec as the InP coverage is increased from 0.8 to 1.5 MLs. Good agreement between experiment and simulations is achieved; the best fit parameters ($d_{\mathrm{GaP}}=42.5$ Å, $d_{\mathrm{InP}}=2.6$, 4.0, and 5.3 Å) agree with the RHEED data as monitored during growth.

[a]Electronic mail: hatami@physik.hu-berlin.de

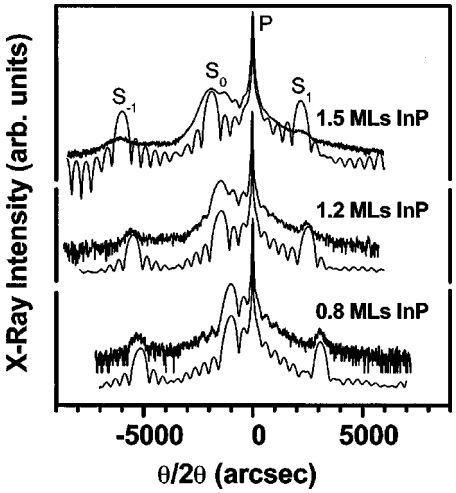

FIG. 1. X-ray rocking curves (004) of InP/GaP superlattices with different InP coverage along with respective simulations (solid lines). The best fits are obtained using $d_{GaP}=42.5$ Å, $d_{InP}=2.6$, 4.0, and 5.3 Å for the lower, middle, and top curves, respectively. With decreasing InP coverage, the zeroth order superlattice satellite (S_0) shifts from -2000 to -1000 arcsec towards the GaP substrate peak (P).

Furthermore, the existence of Pendellösung fringes in the experimental rocking curves reflects the high structural quality of the InP/GaP layers.

Figure 2 shows the PL spectra of three InP/GaP structures. The InP layers in the structures remain 2D because the InP coverage is considerably lower than the critical thickness for island formation.[3] The measurements were carried out at 5 K with an excitation intensity of about 20 W cm^{-2}. The PL emission from the sample with 0.8 MLs of InP consists of four intense PL lines in the energy range of 2.22–2.28 eV with full width at half maximum (FWHM) of 15 ± 2 meV. The total emission intensity grows linearly with increasing excitation power density between 1 and 20 W cm^{-2}. Samples with increased InP coverage have similar emission with all lines redshifted. These PL spectra are also similar to those of $GaAs_xP_{1-x}$/GaP (Refs. 7–9) and AlP/GaP (Ref. 10) type-II quantum wells. The energy differences between the highest energy PL line and the other three transitions are 12, 30, and 40 meV, for all samples.

The energy separations between the peaks and the independence of these separations with respect to InP coverage

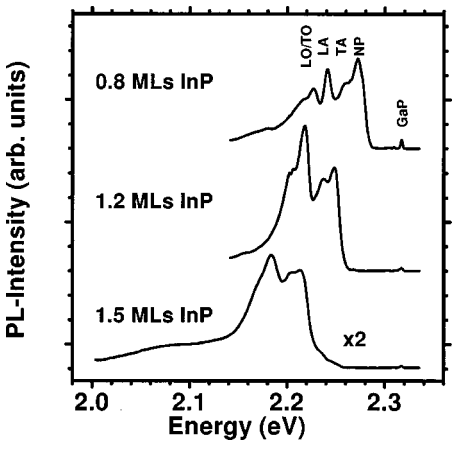

FIG. 2. Photoluminescence spectra of samples with different InP coverage measured at 5 K.

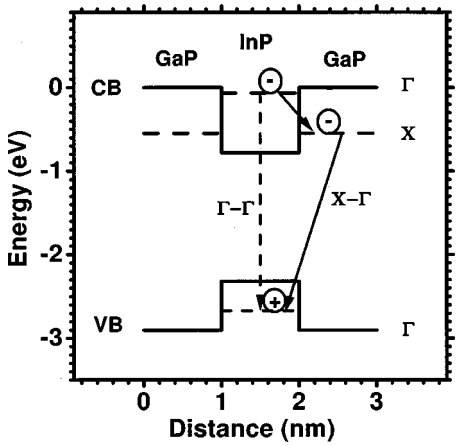

FIG. 3. Valence and conduction band alignment scheme of the InP QW embedded in a GaP matrix. The arrows indicate the two possibilities of electron-hole recombination.

suggest that the three emissions peaks with lower energy are phonon replicas of the highest-lying peak. The separations agree well with the transverse acoustic (TA), longitudinal acoustic (LA), and either transverse optical (TO) or longitudinal optical (LO) phonon near the X points in the GaP Brillouin zone with energies of 13.2, 30.4, and 44–45 meV, respectively.[11,12] These energies are not appreciably changed for $In_yGa_{1-y}P$ with small In mole fraction.[11] Thus, we identify the highest energy peak in each spectrum as the no-phonon (NP) emission and the lower energy peaks as its phonon replicas. In contrast to the similar $GaAs_xP_{1-x}$/GaP system, but with much thicker quantum wells,[8] the relative intensity of this NP line compared to the other three lines does not appear to decrease with the decreasing thickness of the InP layer. In these very thin InP layers, however, the $\Gamma-X$ mixing is probably strongly affected by interface roughness, the interdiffusion of In and Ga, and disorder. The broad emission at the lower energy side of the PL spectrum for the 1.5 ML QW could be related to defects in the highly strained InP 2D layer, which also result in the somewhat decreased total PL intensity compared to structures with thinner InP. Note that island formation already occurs for InP depositions of 1.8 MLs,[3] only 0.3 MLs thicker than this 1.5 ML sample.

The band discontinuity at the interface of a thin InP layer and the (semi-infinite) GaP layer is estimated using the model-solid theory of Van de Walle.[13] Strain has a very significant effect on the conduction and valence band offsets and is also included in this calculation. Figure 3 shows the calculated band alignment for a prototypical structure. We have also calculated the electron to heavy-hole transition energy as function of InP thickness for both the type I (Γ-valley electrons in the first subband of the InP quantum well with heavy holes in the InP) and type II (X-valley electrons in the GaP with heavy holes in the InP) transitions. Our calculations also include the coupling of adjacent InP quantum wells since the superlattice constant ($d_{InP}+d_{GaP}$) is less than 5 nm. The appropriate material parameters are given in Refs. 13 and 14. Within this simple, multivalley effective-mass approximation (EMA), we find that for the InP/GaP heterostructures with InP thickness thinner than about 8 MLs (3 nm), the Γ-like electrons in the InP layer are located at a

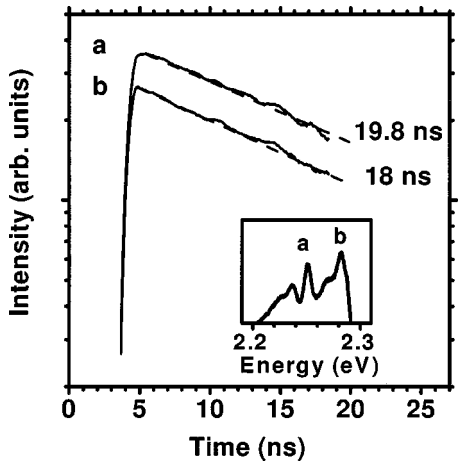

FIG. 4. PL transients from the sample with 0.8 MLs InP coverage. The transients were detected at 2.24 (a) and 2.27 (b) eV and 5 K. The dashed lines show the fit with the corresponding time constant. The inset shows the PL spectrum with the positions of the detection energies marked by a and b.

higher energy than *X* states in the GaP layer and the structure is type II. This calculated energy configuration resembles that of the $GaAs_xP_{1-x}$/GaP system, whose PL spectra are also similar.[7] The same effect has also been observed for essentially unstrained GaAs/AlAs QW structures.[15,16] The type-I transitions are calculated to have energies exceeding 2.7 eV for InP coverage of under 2 MLs, while the calculated type-II transitions lie between 2.25 and 2.35 eV. Figure 2 shows measured energies of the NP transitions are between 2.2 and 2.3 eV, in very good agreement with the calculated type-II transitions and much lower than the calculated type-I transitions.

In order to investigate the dynamics of carrier recombination in InP/GaP heterostructures, we performed time-resolved PL measurements at 5 K. The transients exhibit an exponential decay with a decay time of 19 ± 1 ns detected at different energies (NP, TA, LA, LO), which is nearly independent of the InP coverage in the range of 0.8–1.5 MLs. Figure 4 shows the PL transients from the sample containing 0.8 MLs InP layers. The transients were detected at 2.24 (a) and 2.27 (b) eV. The dashed lines show the fit with the corresponding time constant. The results from time-resolved PL further confirm our band alignment modeling. Compared to the carrier lifetime in a thin strained type-I system of about 100 ps,[17] the significantly longer carrier lifetime for ultrathin InP/GaP QWs can be explained by a type-II band alignment in this system.

To conclude, we have described the growth and optical investigation of ultrathin InP QWs on (100) GaP. Intense PL from the structures is observed between 2.17 and 2.28 eV. The PL is explained as resulting from the spatially indirect recombination of electrons from the GaP *X* valleys with holes in InP and its phonon replicas. The highest energy NP line of each PL spectrum can be well explained using a realistic EMA calculation based on a type-II band alignment. The type-II band alignment is further confirmed by the carrier lifetime of about 19 ns, which is much longer than in type-I systems.

[1] W. D. Laidig, Y. F. Lin, and P. J. Caldwell, J. Appl. Phys. **57**, 33 (1985).
[2] A. Ketterson, M. Moloney, W. T. Masselink, J. Klem, R. Fischer, W. Kopp, and H. Morkoç, IEEE Electron Device Lett. **EDL-6**, 628 (1985).
[3] F. Hatami, L. Schrottke, and W. T. Masselink, Appl. Phys. Lett. **78**, 2163 (2001).
[4] F. Hatami, U. Müller, H. Kissel, K. Braune, R-P. Blum, S. Rogaschewski, H. Niehus, H. Kirmse, W. Neumann, M. Schmidbauer, R. Köhler, and W. T. Masselink, J. Cryst. Growth **216**, 26 (2000).
[5] H. Schmidt, B. Rheinländer, V. Gottschalch, and G. Wagner, Thin Solid Films **312**, 356 (1998).
[6] J. N. Baillargeon, K. C. Hsieh, and G. E. Stillman, J. Appl. Phys. **68**, 2133 (1990).
[7] J. A. Prieto, G. Armelles, M.-E. Pistol, P. Castrillo, J. P. Silveira, and F. Briones, Appl. Phys. Lett. **70**, 3449 (1997).
[8] M.-E. Pistol, M. R. Leys, and L. Samuelson, Phys. Rev. B **37**, 4664 (1988).
[9] K. Arimoto, T. Sugita, N. Usami, and Y. Shiraki, Phys. Rev. B **60**, 13735 (1999).
[10] S. Nagao, T. Fujimori, H. Gotoh, H. Fukushima, T. Takano, H. Ito, S. Koshihara, and F. Minami, J. Appl. Phys. **81**, 1417 (1997).
[11] P. Merle, D. Auvergne, and H. Mathieu, Phys. Rev. B **15**, 2032 (1977).
[12] H. Mathieu, P. Merle, and E. L. Ameziane, Phys. Rev. B **15**, 2048 (1977).
[13] C. Van de Walle, Phys. Rev. B **39**, 1871 (1989).
[14] *Physics of Group IV Elements and III–V Compounds*, edited by O. Madelung, M. Schulz, and H. Weiss, Landolt-Börnstein Numerical Data and Relationships, New Series **III**, 17a (Springer, Berlin, 1982).
[15] J. Moore, G. Duggan, P. Dawson, and C. T. Foxon, Phys. Rev. B **38**, 5535 (1988).
[16] J. Feldmann, R. Sattmann, E. Göbel, J. Kuhl, J. Hebling, K. Ploog, R. Muralidharan, P. Dawson, and C. T. Foxon, Phys. Rev. Lett. **62**, 1892 (1989).
[17] Yu. I. Mazur, J. W. Tomm, V. Petrov, G. G. Tarasov, H. Kissel, C. Walther, Z. Ya. Zhuchenko, and W. T. Masselink, Appl. Phys. Lett. **78**, 3214 (2001).